EXPERIMENTAL EVALUATION OF R1336MZZ(Z) AS LOW GWP REPLACEMENT FOR R245FA IN A SCROLL EXPANDER

Matthias Welzl*, Florian Heberle, Theresa Weith, Dieter Brüggemann

University of Bayreuth,
Chair of Engineering Thermodynamics and Transport Processes (LTTT),
Center of Energy Technology (ZET)
Bayreuth, Germany
matthias.welzl@uni-bayreuth.de

* Corresponding Author

ABSTRACT

Hydrofluoroolefin (HFO) refrigerants are promising low global warming potential (GWP) alternatives to the currently used hydrofluorocarbons (HFCs) in Organic Rankine Cycle (ORC) systems. This study led the focus on the experimental evaluation of the novel HFO R1336mzz(Z) as a low GWP replacement for the HFC R245fa. The investigated scroll expander is a semi-hermetic oil-free expander with a rated power of 1 kW and a built-in volume ratio of 3.5, which is magnetically coupled with a 1 kW permanently excited synchronous generator. For the determination of the expander mechanical power output, a contactless torque sensor is integrated. The experimental investigation involved measurements at eight different operating conditions for the working fluids R245fa and R1336mzz(Z), varying the saturation temperature, the scroll expander rotational speed, and the pressure ratio. The maximum mechanical isentropic efficiencies of 58.9 % for R245fa and 57.0 % for R1336mzz(Z) were obtained at a saturation temperature of 90 °C. For all variations, the mechanical isentropic efficiency for R1336mzz(Z) is between 0.9 % and 6.2 % lower compared to R245fa. The experimental evaluation indicates, that R1336mzz(Z) is a suitable low GWP replacement for R245fa with slightly lower scroll expander efficiencies.

1. INTRODUCTION

Hydrofluoroolefin (HFO) refrigerants have received much attention in recent years due to their low global warming potential (GWP) in combination with low flammability and low toxicity. HFOs are therefore promising alternatives to the hydrofluorocarbons (HFCs) with their high GWP which are currently used in Organic Rankine Cycle (ORC) systems. The consumption of these HFCs is globally being reduced according to the Kigali Amendment of the Montreal Protocol (United Nations Environment Programme, 2016). In the European Union (EU), the available quantity of HFCs in 2018 has been set to 63 % of the initial quantity of CO_2 equivalents under the EU F-Gas regulation (The European Parliament and the Council of the European Union, 2014), which has led to a sharp increase in prices for HFCs. To replace currently used HFC working fluids by HFOs, a comprehensive experimental evaluation of the expander operation is needed. In small-scale ORC systems in geothermal, solar power, and waste heat recovery applications, volumetric expanders are suitable expansion machines (Quoilin et al., 2013). The performance of these expanders is strongly determined by the operating parameters and the thermophysical properties of the working fluid.

In current literature, the focus is led on the experimental evaluation of the complete ORC system with a given heat source and sink. Molés et al. (2016) evaluated the hydrochlorofluoroolefin (HCFO) R1233zd(E) as a replacement for R245fa in an ORC for low-temperature heat sources using a scroll expander. Navarro-Esbrí et al. (2017) investigated with the same commercial ORC module the HFO R1336mzz(Z) as a replacement for R245fa. They varied the heat source (thermal oil) and heat sink (water) temperature in a wide range, keeping the volume flow rate constant. In both studies, higher expander electrical isentropic efficiencies were observed for the low GWP working fluids. Eyerer et al. (2019) carried out investigations for the HCFOs R1233zd(E) and R1224yd(Z) as replacements for R245fa in ORC systems. During all experiments the heat source (water) parameters were kept constant, varying the working fluid mass flow rate, condensing temperature, and expander rotational speed. The authors proposed that the electrical isentropic efficiencies of the lubricated semi-hermetic scroll expander are not significantly influenced by the working fluid properties, but mainly by fluid dependent operating parameters such as supply pressure and volume flow rate. Yang et al. (2018) compared R1233zd(E) to R245fa for ORC applications using an open-drive scroll expander, which was modified from a commercial compressor. In a further study, an experimental comparison of R245fa to its alternatives R1234ze(Z), R1233zd(E), and R1336mzz(E) was performed using a lubricated hermetic scroll expander (Yang et al., 2019). The temperatures and volume flow rates of the thermal oil heating loop and the water cooling loop were kept constant, while the working fluid mass flow rate and the expander rotational speed were varied. The authors concluded that R1234ze(Z) and R1233zd(E) are appropriate drop-in replacements for R245fa, whereas R1336mzz(E) shows extremely lower thermal efficiencies.

Few studies have concentrated on a systematic investigation of the scroll expander efficiency when replacing the HFC working fluid by HFOs. Therefore, it is necessary to determine the mechanical isentropic efficiency of the expander while performing experiments under comparable operating conditions for the different working fluids.

In this study, the focus is led on the experimental evaluation of a scroll expander using the novel HFO R1336mzz(Z) as a low GWP replacement for the HFC R245fa. The investigated scroll expander is a modified 1 kW semi-hermetic type by Air-Squared Inc. with a built-in volume ratio of 3.5. Experiments were carried out for both working fluids varying the saturation temperature, the scroll expander rotational speed, and the pressure ratio. Based on these results, the scroll expander operation is evaluated, applying the mechanical isentropic efficiency as a performance indicator. Furthermore, the influence of the generator efficiency on electrical isentropic efficiency is considered.

2. EXPERIMENTAL INVESTIGATIONS

2.1 Comparison of working fluids

In Table 1, a comparison of the fluid properties of R245fa and R1336mzz(Z) is shown. The listed thermophysical properties are based on REFPROP 10.0 (Lemmon et al., 2018). In particular, the GWP of R1336mzz(Z) is significantly lower compared to R245fa. Furthermore, both working fluids show no ozone depletion potential (ODP), in contrast to HCFOs as possible replacements for HFCs.

Table 1: Fluid properties of the investigated working fluids.

Parameter	R245fa	R1336mzz(Z)
Chemical name	1,1,1,3,3-pentafluoropropane	cis-1,1,1,4,4,4-hexafluoro-2-butene
Chemical formula	$CHF_2CH_2CF_3$	$CF_3CH{=}CHCF_3$
CAS number	460-73-1	692-49-9
Safety group (ASHRAE, 2016)	B1	A1
GWP 100 year (Hodnebrog et al., 2013, Myhre et al., 2013)	858	2
ODP	0	0
Molar mass (g/mol)	134.05	164.06
Critical pressure (MPa)	3.651	2.903
Critical temperature (K)	427.01	444.5
Normal boiling point temperature (K)	288.2	306.6

2.2 Description of the test rig

The working fluids were investigated with an ORC test rig, shown in Figure 1. As a heat source, the electrical heated preheater and evaporator can be used. Inside the evaporator, a heating element instrumented with eight Pt100 is mounted for the simultaneous determination of nucleate pool boiling heat transfer coefficients (Welzl et al., 2018). The saturated vapour leaving the evaporator can be expanded either with the throttle valve or with the scroll expander, depicted in Figure 2.

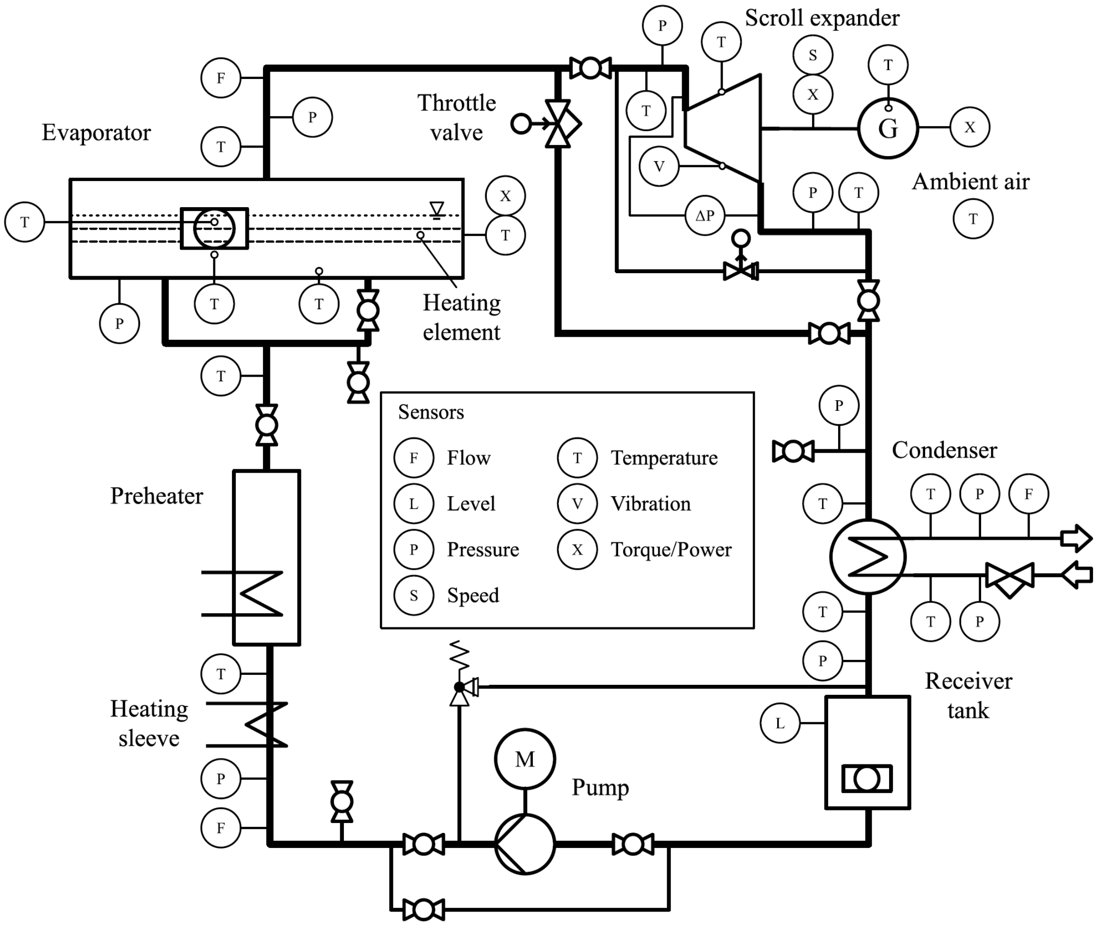

Figure 1: Scheme of the ORC test rig.

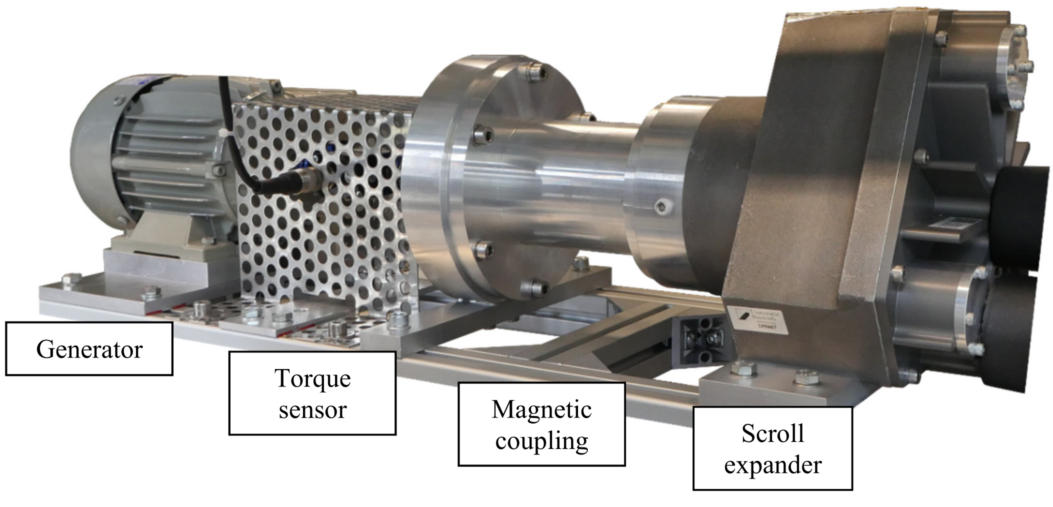

Figure 2: Photograph of the scroll expander.

The investigated scroll expander E15H022A-SH, manufactured by Air Squared Inc., is a semi-hermetic expander with a rated power of 1 kW, a built-in volume ratio of 3.5, and a swept volume of 14.5 cm³. The expander is operated without lubricant and is connected by magnetic coupling with a 1 kW permanently excited synchronous generator (Huebner Giessen DSG P) for electrical power generation. For the determination of the expander mechanical power output, a contactless torque sensor with integrated rotational speed measurement is used. A commercial variable electronic load is integrated to control the scroll expander rotational speed and measure the electrical power output. After expansion, the working fluid is condensed in a brazed plate heat exchanger, cooled by water. The volume flow rate of the cooling water can be adjusted by a valve to set the condensing pressure and thus the pressure ratio of the scroll expander. Finally, the condensed working fluid is fed from the receiver tank to the preheater by a piston diaphragm pump.

2.3 Data evaluation and measurement devices

For the evaluation of the experimental data, the following equations are used. The pressure ratio r_p of supply pressure p_{su} to exhaust pressure p_{ex} of the scroll expander is defined as:

$$r_p = p_{su} / p_{ex} . \tag{1}$$

The mechanical power output of the scroll expander P_{mech} is calculated with the measured shaft torque M and the rotational speed n:

$$P_{mech} = 2\pi M n. \tag{2}$$

The mechanical isentropic efficiency $\eta_{s,mech}$ as a performance indicator of the scroll expander is defined as the ratio of mechanical power to isentropic expansion power:

$$\eta_{s,mech} = \frac{P_{mech}}{\dot{m}_{wf}\left(h_{su} - h_{s,ex}\right)}. \tag{3}$$

The isentropic expansion power is calculated with the measured working fluid mass flow rate $\dot{m}_{wf}$, the supply enthalpy h_{su}, and the isentropic exhaust enthalpy $h_{s,ex}$ of the scroll expander. These enthalpies are determined with measured supply and exhaust pressures and the supply temperature by REFPROP 10.0 (Lemmon et al., 2018). The measured electrical power output P_{el} includes the generator losses and is used to calculate the electrical isentropic efficiency $\eta_{s,el}$ of the scroll expander:

$$\eta_{s,el} = \frac{P_{el}}{\dot{m}_{wf}\left(h_{su} - h_{s,ex}\right)}. \tag{4}$$

The filling factor ϕ, indicating internal leakages, is calculated as

$$\phi = \frac{\dot{m}_{wf} v_{su}}{n V_s} \tag{5}$$

with the specific volume of the working fluid at the supply v_{su} and the swept volume of the scroll expander V_s. The measurement devices for data acquisition and its accuracies are listed in Table 2.

Table 2: Accuracy of measurement devices.

Measured parameter	Measurement device	Accuracy of device
Scroll expander torque M	Torque sensor	±5 mNm
Scroll expander rotational speed n	Torque sensor	±50 ppm n
Generator electrical power P_{el}	Electronic load	±2.4 W
Working fluid mass flow rate $\dot{m}_{wf}$	Coriolis sensor	$\pm\left(0.1\ \% + 0.2\ \text{kg/h}/\dot{m}_{wf}\right)\dot{m}_{wf}$
Working fluid supply pressure p_{su}	Piezoresistive pressure sensor	±35 mbar
Working fluid exhaust pressure p_{ex}	Piezoresistive pressure sensor	±14 mbar
Working fluid supply temperature T_{su}	Pt100	$\pm\left(0.1\ °\text{C} + 0.0017\lvert T_{su}\rvert\right)$

2.4 Methodology

The current investigation involved measurements at eight different operating conditions for the working fluids R245fa and R1336mzz(Z). The experiments were carried out for the operating parameters shown in Table 3. For each operating parameter, a variation was performed in which the other parameters remained constant at the reference values. In order to acquire the measurement data for each operating condition a period of ten minutes of steady state operation was maintained. To ensure that stationarity was achieved, the receiver tank level, the working fluid mass flow rate and the inlet and outlet pressure of the scroll expander had to be constant. The measured values were logged every second and averaged over the test period for data reduction.

Table 3: Experimental operating parameters.

Operating parameter	Reference value	Parameter variation
Saturation temperature T_{sat} (°C)	80	70, 90
Scroll expander rotational speed n (rpm)	3000	2700, 3300
Pressure ratio r_p (-)	3.5	3, 4, 4.5

3. RESULTS AND DISCUSSION

3.1 Variation of the saturation temperature

The mechanical and electrical isentropic efficiencies in Figure 3 (a) illustrates the findings of the saturation temperature variation for a rotational speed of 3000 rpm and a pressure ratio of 3.5. Figure 3 (b) shows the mechanical and electrical expander power output as a function of the working fluid mass flow rate.

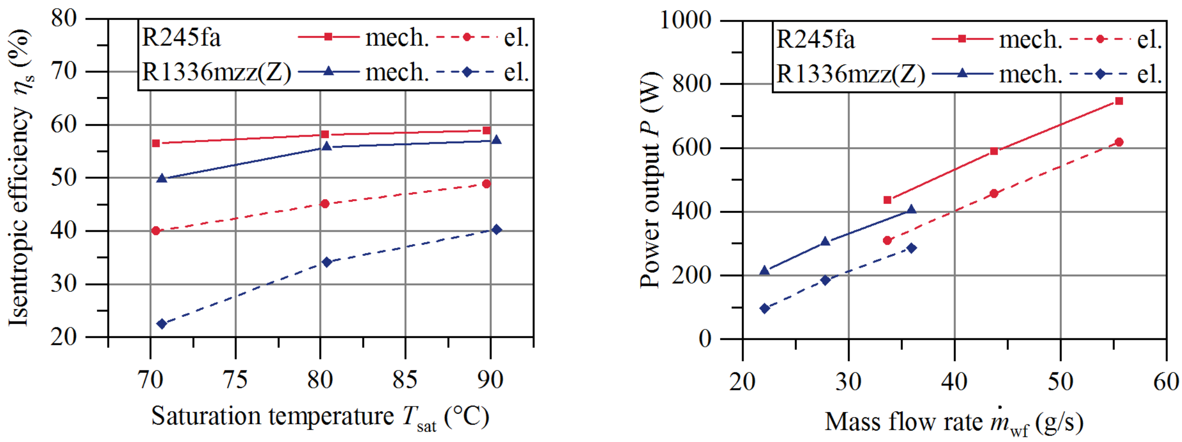

(a) (b)

Figure 3: (a) Isentropic efficiency depending on saturation temperature; (b) Power output as a function of working fluid mass flow rate.

The variation of the saturation temperature corresponds to a scroll expander supply temperature and pressure variation. It can be seen, that the efficiencies and power outputs increase with higher saturation temperatures and mass flow rates. The mechanical isentropic efficiency is in a range between 49.8 % and 58.9 %, which is in good accordance to reported efficiencies for oil-free scroll expander in literature (Quoilin et al., 2013). In comparison, R1336mzz(Z) shows a lower mechanical isentropic efficiency than R245fa. This can be explained by increased internal leakage of R1336mzz(Z), caused by different thermophysical properties. The resulting mass flow rate of R1336mzz(Z) and therefore the power output is lower due to the lower vapour density at the given saturation temperature. The characteristic of electrical isentropic efficiency, with a maximum value of 48.8 % for R245fa, indicates the influence of the generator efficiency, especially for low power outputs.

3.2 Variation of the scroll expander rotational speed

Figure 4 (a) and (b) demonstrate the influence of the scroll expander rotational speed on the isentropic efficiencies and power outputs for a saturation temperature of 80 °C and a pressure ratio of 3.5.

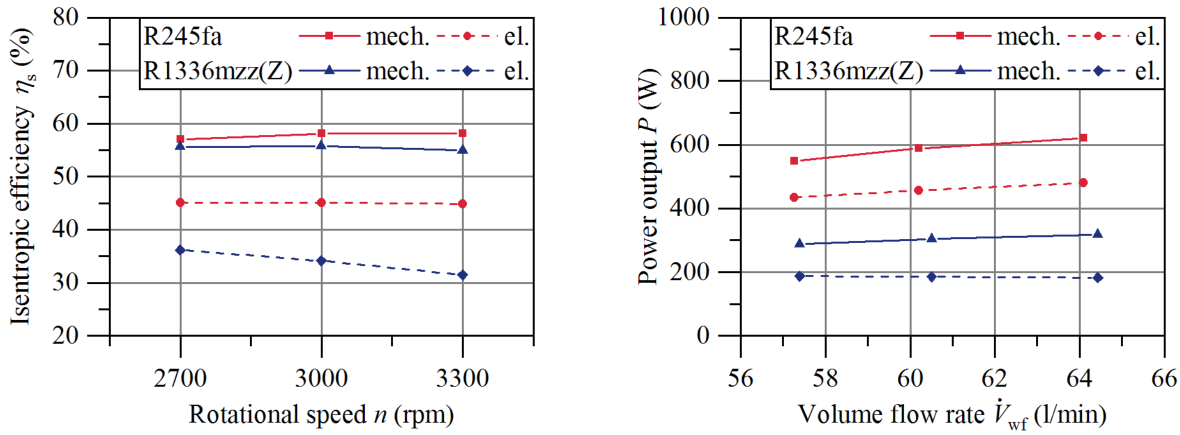

(a) (b)

Figure 4: (a) Isentropic efficiency depending on rotational speed; (b) Power output as a function of working fluid volume flow rate.

An increasing rotational speed leads to a higher volume flow rate at constant saturation temperature. The mechanical isentropic efficiencies are slightly lower for R1336mzz(Z) with a maximum absolute difference of -3.1 % compared to R245fa. Again, this difference can be explained with higher internal leakages indicated by the higher volume flow rates of R1336mzz(Z) at equal rotational speed as shown in Figure 4 (b). The electrical isentropic efficiency for R1336mzz(Z) demonstrates the distinctive rotational speed dependency of the generator efficiency. A higher rotational speed leads to higher losses mainly caused by the internal fan of the generator.

3.3 Variation of the pressure ratio

In Figure 5 (a) and (b) isentropic efficiencies and power outputs are compared under variation of the pressure ratio at a saturation temperature of 80 °C and a rotational speed of 3000 rpm.

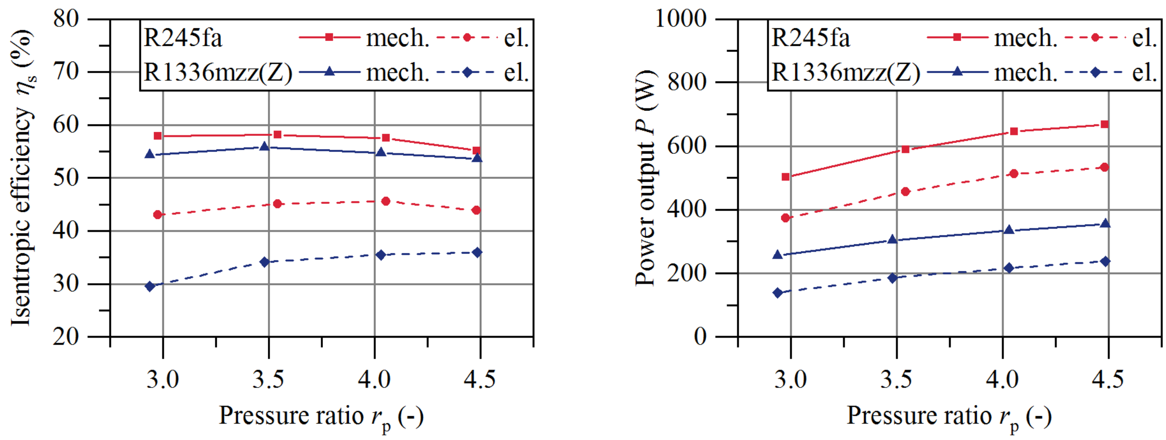

(a) (b)

Figure 5: (a) Isentropic efficiency depending on pressure ratio; (b) Power output as a function pressure ratio.

The highest mechanical isentropic efficiency of 55.7 % for R1336mzz(Z) and 58.1 % in case of R245fa can be observed at a pressure ratio of 3.5, which corresponds approximately to a volume ratio of 3.5. This is consistent with additional losses due to under- or over-expansion for pressure ratios that are not in the range of the built-in volume ratio of 3.5. The mechanical isentropic efficiency is lower for R1336mzz(Z). The reason for this is illustrated in Figure 6. The higher filling factor for R1336mzz(Z) indicates a higher internal leakage, which could be caused by lower vapour viscosities. Furthermore, the increase in filling factor with a higher pressure ratio is in good agreement with theory.

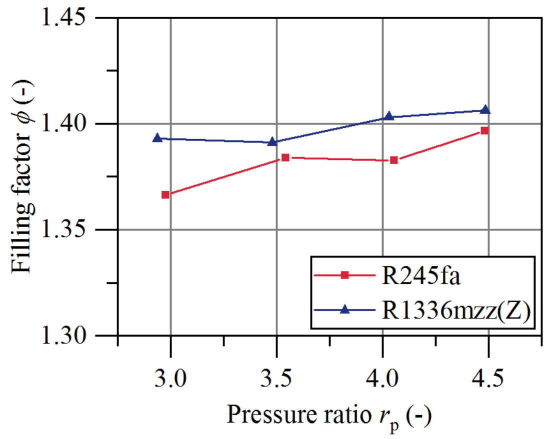

Figure 6: Filling factor as a function of pressure ratio.

3.4 Generator efficiency

It is evident from the presented experimental results that the generator efficiency has a crucial impact on electrical isentropic efficiency and power output. In Figure 7 the generator efficiency is shown as a function of the generator load for all measurements at a rotational speed of 3000 rpm.

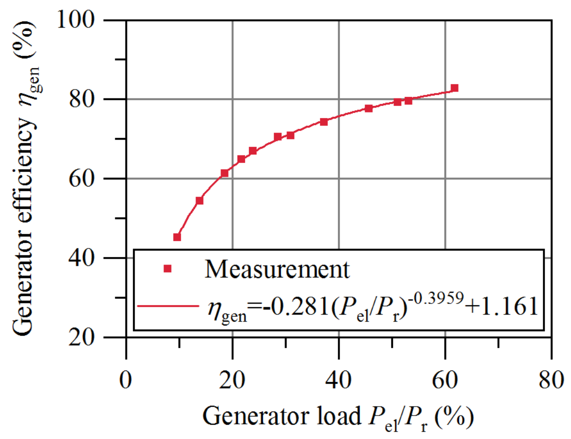

Figure 7: Generator efficiency as a function of the generator load at a rotational speed of 3000 rpm.

The generator load, defined as the ratio between the measured electrical power and the rated power of the generator P_r, has been in a range from 9.6 % to 61.8 %. For this operational range, a power-law fit is provided with an RMSE of 0.005. It can be seen that the generator efficiency increases with load and is in particular sensitive at small loads. Therefore, it is important to determine the mechanical power output for the experimental evaluation of a scroll expander when using different working fluids in a wide power range. The described fit can be applied to estimate the influence of the generator efficiency on the expander electrical isentropic efficiency for similar generator types without torque measurment.

4. CONCLUSIONS

In this study, a scroll expander was investigated using the novel HFO refrigerant R1336mzz(Z) as a low GWP replacement for R245fa. The focus of the experiments was led on comparable scroll expander operating conditions for both working fluids. In order to evaluate the scroll expander performance, the mechanical isentropic efficiency is chosen as an indicator. The highest mechanical isentropic efficiencies were obtained at the highest saturation temperature of 90 °C close to the built-in volume ratio. The maximum value is 58.9 % with R245fa and 57.0 % with R1336mzz(Z). For all variations, the mechanical isentropic efficiency with R1336mzz(Z) is lower compared to R245fa. The relative difference based on the efficiency of R245fa is between -0.9 % and -6.2 %. The reason for this is a higher internal leakage as indicated by a higher filling factor for R1336mzz(Z). The generator efficiency has a significant impact on electrical isentropic efficiency and power output and should be considered for comparisons. In summary, R1336mzz(Z) is a suitable low GWP replacement for R245fa with slightly lower scroll expander efficiencies. An important question for future studies is to determine the influence of the thermophysical working fluid properties on expander efficiency.

REFERENCES

ASHRAE, 2016, Designation and Safety Classification of Refrigerants, Standard 34-2016.

Eyerer, S., Dawo, F., Kaindl, J., Wieland, C., Spliethoff, H., 2019, Experimental investigation of modern ORC working fluids R1224yd(Z) and R1233zd(E) as replacements for R245fa, *Applied Energy*, vol. 240: p. 946-963.

Hodnebrog, Ø., Etminan, M., Fuglestvedt, J. S., Marston, G., Myhre, G., Nielsen, C. J., Shine, K. P., Wallington, T. J., 2013, Global warming potentials and radiative efficiencies of halocarbons and related compounds: A comprehensive review, *Rev. Geophys.*, vol. 51, no. 2: p. 300-378.

Lemmon, E. W., Bell, I. H., Huber, M. L., McLinden, M. O., 2018, NIST Standard Reference Database 23: Reference Fluid Thermodynamic and Transport Properties-REFPROP, Version 10.0, *National Institute of Standards and Technology.*

Molés, F., Navarro-Esbrí, J., Peris, B., Mota-Babiloni, A, 2016, Experimental evaluation of HCFO-1233zd-E as HFC-245fa replacement in an Organic Rankine Cycle system for low temperature heat sources, *Applied Thermal Engineering*, vol. 98: p 954-961.

Myhre, G., Shindell, D., Bréon, F.-M., Collins, W., Fuglestvedt, J., Huang, J., Koch, D., Lamarque, J.-F., Lee, D., Mendoza, B., Nakajima, T., Robock, A., Stephens, G., Takemura, T., Zhang, H, 2013, Anthropogenic and Natural Radiative Forcing, *In*: Stocker, T. F., Qin, D., Plattner, G.-K., Tignor, M., Allen, S. K., Boschung, J., Nauels, A., Xia, Y., Bex, V., Midgley, P. M., *Climate change 2013: The physical science basis: Working Group I contribution to the Fifth assessment report of the Intergovernmental Panel on Climate Change*, Cambridge University Press, Cambridge, United Kingdom, New York, NY, USA: p. 659-740.

Navarro-Esbrí, J., Molés, F., Peris, B., Mota-Babiloni, A., Kontomaris, K., 2017, Experimental study of an Organic Rankine Cycle with HFO-1336mzz-Z as a low global warming potential working fluid for micro-scale low temperature applications, *Energy*, vol. 133: p. 79-89.

Quoilin, S., van den Broek, M., Declaye, S., Dewallef, P., Lemort, V., 2013, Techno-economic survey of Organic Rankine Cycle (ORC) systems, *Renewable and Sustainable Energy Reviews*, vol 22: p. 168-186.

The European Parliament and the Council of the European Union, 2014, Regulation (EU) No 517/2014 of the European Parliament and of the Council of 16 April 2014 on fluorinated greenhouse gases and repealing regulation (EC) No 842/2006.

United Nations Environment Programme, 2016, Amendment to the Montreal Protocol on Substances that Deplete the Ozone Layer, Kigali.

Welzl, M., Heberle, F., Brüggemann, D., 2018, Experimental evaluation of nucleate pool boiling heat transfer correlations for R245fa and R1233zd(E) in ORC applications, *Renewable Energy*, doi: 10.1016/j.renene.2018.09.093.

Yang, J., Sun, Z., Yu, B., Chen, J., 2018, Experimental comparison and optimization guidance of R1233zd(E) as a drop-in replacement to R245fa for organic Rankine cycle application. *Applied Thermal Engineering*, vol. 141: p. 10-19.

Yang, J., Ye, Z., Yu, B., Ouyang, H., Chen, J. Simultaneous experimental comparison of low-GWP refrigerants as drop-in replacements to R245fa for Organic Rankine cycle application: R1234ze(Z), R1233zd(E), and R1336mzz(E), *Energy*, vol. 173: p. 721-731.

ACKNOWLEDGEMENT

The samples of R245fa and R1336mzz(Z) were kindly donated by Honeywell Deutschland GmbH and The Chemours Company FC, LLC. Funding from the Bavarian State Ministry of Education, Science and the Arts in the framework of the project "Geothermie-Allianz Bayern" is gratefully acknowledged.